Influence of Pyrolysis Conditions on the Properties and Pb^{2+} and Cd^{2+} Adsorption Potential of Tobacco Stem Biochar

Xiaopeng Wang,[a,b,†] Muhammed Mustapha Ibrahim,[a,b,d,†] Chenxiao Tong,[a,b] Kun Hu,[a,b] Shihe Xing,[a,b] and Yanling Mao [a,b,c,*]

Converting biomass into biochar is a smart recycling strategy. Biochar was produced from tobacco stems at temperatures of 400 °C, 500 °C, 600 °C, and 700 °C and holding times of 1.5 h, 2 h, 2.5 h, and 3 h. Its properties and adsorption capacities for Pb^{2+} and Cd^{2+} were evaluated. While the yield decreased, pH, phosphorus, potassium, ash, and surface area increased with increasing pyrolysis temperature and holding time. Nitrogen, volatile matter, and pore diameter decreased as the temperature increased, with an irregular effect of the holding time. A peak C content (652 g/kg) was recorded at 600 °C (2 h). The highest values obtained for the N, P, and K content were 25.6 g/kg (400 °C and 2 h), 7.82 g/kg and 168 g/kg (600 °C and 3 h), respectively. The heavy metal contents were within tolerable limits. The highest surface and micropore areas of 50.6 and 57.1 m^2g^{-1}, respectively, were obtained at 700 °C (3 h). The biochar had a wide range of aliphatic and aromatic C functional groups. The highest adsorption percentages of Pb^{2+} and Cd^{2+} (44.5 % and 38.3 %, respectively) by biochar produced at 700 °C (3 h) signified its suitability for heavy metal adsorption. These properties made the biochar a suitable soil amendment.

Keywords: Tobacco stem; Recycling; Biochar; Heavy metals; Adsorption

Contact information: a: College of Resources and Environment, Fujian Agriculture and Forestry University, Fuzhou, Fujian Province 350002 China; b: Key Research Laboratory of Soil Ecosystem Health and Regulation in Fujian Provincial University, Fuzhou, Fujian Province 350002 China; c: Fujian Colleges and Universities Engineering Research Institute of Conservation and Utilization of Natural Bioresources, College of Forestry, Fujian Agriculture and Forestry University, Fuzhou, Fujian Province 350002 China; d: Department of Soil Science, University of Agriculture, Makurdi 972211 Nigeria
** Corresponding author: fafum@126.com; † Equal contribution by authors*

INTRODUCTION

Agricultural activity in China produces a large quantity, variety, and distribution of biomass resources. As a widely grown cash crop in China, tobacco has a unique economic value (Zhang 2002). The total area of the annual tobacco crops grown in China is reported to be approximately 1 million hectares, with an annual output of 2.36 million tons of tobacco leaves (Sun *et al.* 2016). When comparing the ratio of the tobacco stem (rod) to the tobacco leaves produced at harvest, the annual tobacco stem output is higher. The efficient use of tobacco as biomass has not been fully explored, as it is considered residue after harvest, as well as having a hard texture. After the tobacco leaves are harvested, the tobacco stem becomes a source of waste. They are either discarded as a solid waste or locally incinerated, therefore contributing to air pollution (Wang 2007).

The accumulation of agricultural wastes and their disposal *via* burning constitutes an environmental problem of global concern (Sobati *et al.* 2016). The burning of tobacco crop residue is a key source of air-borne carbonaceous aerosols, which is highly hazardous to the health of both humans and the ecosystem in China (Zhang *et al.* 2013). Options for disposing of the increasing quantity of these residues poses a serious challenge for agriculture in China. It is therefore of utmost importance to find a suitable alternative recycling method for tobacco stems, which may have potential as a high value-added product. Research on the utilization of hard agricultural waste, *e.g.*, straw and woody biomass, primarily focuses on the manufacturing of fuel, the extraction of raw chemical materials, and papermaking (Yan *et al.* 2008).

The conversion of agricultural wastes into biochar has been proposed as an effective means of handling agricultural wastes (Kuzyakov *et al.* 2014). Biochar refers to the carbon-rich organic material obtained when biomass is heated to temperatures greater than 250 °C under oxygen-limited conditions (Lehmann and Joseph 2015). The application of biochar in soil has shown great potential in terms of crop production, capturing greenhouse gases, and improving soil properties (Kang 2018). The porous structure and high carbon content of biochar influence its physical and chemical properties, *e.g.*, its high stability and strong adsorption (O'Laughlin and McElligott 2009). Therefore, the incorporation of biochar into the soil can also produce a number of important ecological benefits: increasing the soil fertility and improving agricultural production (Anna and Patryk 2015; Subedi *et al.* 2016); as a bacterial inoculant carrier (Egamberdiva *et al.* 2018); capturing greenhouse gases (Mechler *et al.* 2018); increasing the soil carbon stocks; and reducing the risk of contaminants and heavy metals in the soil (Beiyuan *et al.* 2017; Wang et *al.* 2017; Yoo *et al.* 2018), in addition to several other applications.

Unlike other types of anthropogenic-induced pollutants, heavy metals are non-degradable and can therefore only be removed from the environment *via* remediation (Ahmad *et al.* 2018). Biochar has been widely used as an adsorbent for the removal of contaminants due to the numerous functional groups present on its surface (*e.g.* alkyl, hydroxyl, carbonyl, carboxyl, alkyne, amide, *etc*.) and developed pore structure (Ahmad *et al.* 2018; Li *et al.* 2019). However, sorption of ions is a complex characteristic of biochar that is difficult to predict (Pignatello *et al.* 2017), due to the varying properties of biochar prepared using different feedstock and production conditions. Therefore evaluating the properties and sorption potentials of biochar produced from tobacco stems will be useful to provide its alternative uses in environmental management.

The pyrolysis conditions, *i.e.*, the temperature and holding time, and the nature of feedstock biomass are important factors that determine the properties of the derived biochar and can therefore influence its environmental application (Sun *et al.* 2014). However, detailed information on the properties of tobacco stem biochar and how it can influence its application has not received sufficient research. This poses a major research gap in the exploration of the usage of agricultural waste products as biochar. Its conversion into biochar and exploring its unique properties will pave way for determining any potential alternative uses. For this study, tobacco stems were collected and used to produce biochar under different conditions (temperatures and holding times), and the nutritional and elemental composition, structure and surface characteristics, and Pb^{2+} and Cd^{2+} adsorption potential of each biochar was studied.

EXPERIMENTAL

Materials

Preparation of biochar

The tobacco stem (variety Cuibi No. 1) was obtained from the Fujian Tobacco Agricultural Science Research Institute (Fujian, China). The stems were air-dried, crushed, and passed through a 1 mm sieve. Before pyrolysis, the sample was placed in an oven at 70 °C for 24 h to reduce the moisture content to approximately 7%. After weighing the biomass, slow pyrolysis was carried out using a biomass carbonizer (SSBP-50004, Biomass Technology Co. Ltd, Jiangsu, China). Nitrogen gas was introduced for 5 min to remove the internal oxygen prior to pyrolysis. The feedstock was pyrolyzed at a heating rate of 10 °C/min at temperatures of 400 °C, 500 °C, 600 °C, and 700 °C, and for each of the carbonization temperatures a holding time of 1.5 h, 2 h, 2.5 h, and 3 h was used. The carbonized sample was left to cool at room temperature, taken out, and then ground through a 0.149 mm sieve for subsequent characterization.

Methods

Biochar characterization

The biochar yield was estimated under a dry ash free (daf) basis with the following relationship, as shown in Eq. 1 and Eq. 2,

$$Y_{biochar};\ daf = 100\ x\ (Y_{biochar} - A) / (100 - M - A) \quad (1)$$

$$Y_{biochar};\ ad = 100\ x\ M_{biochar} / M_{biomass} \quad (2)$$

where $M_{biochar}$ (wt%) represents the weight of the biochar, $Y_{biochar}$; *ad* (wt%) represents the air-dried biochar yield, $M_{biomass}$ represents the weight of the biomass, and *M* and *A* (wt%) represent the moisture and ash content of the biomass, respectively.

Using ASTM E1755-01 (2015), the ash content was determined by the mass loss after the combustion of the dry biochar samples in an open crucible placed in a muffle furnace for 4 h at 700 °C. The determination of the total amount of volatile matter was performed by measuring the weight loss before and after the combustion of 1 g of biochar in a crucible at 950 °C (Li *et al.* 2018).

The pH of the samples was determined by weighing 0.5 g of biochar and placing it into a centrifuge tube. Then, 10 mL of distilled water was added (at a ratio of 1:20, by w:v) and shaken at 150 rpm for 24 h at room temperature (Jindo *et al.* 2014). The pH was measured using a pH meter (PHS-3E, INESA Scientific Instrument Co., Ltd., Shanghai, China).

The carbon (C) and nitrogen (N) contents of the biochar were determined *via* an elemental analyzer (VarioMax; Elementar, Lagenselbold, Germany). The total phosphorus (P) and potassium (K) content were determined using the APHA standard 4500-P (1992). The total P concentration was measured using the vanadium molybdenum yellow colorimetric method and the total K was measured using a flame atomic spectroscopy (FP640, AOPU Analytical Instruments, Shanghai, China). The available P was determined using the Olsen [sodium bicarbonate (NaHCO3)] extracting solution method. The extract was analyzed for P colorimetrically. Available K was measured by weighing 1 g of biochar into a 50 mL Erlenmeyer flask, and 25 mL of 1 $mol \cdot L^{-1}$ NH_4OAc solution was added and shook at 25 ^oC for 30 min, filtered, and measured using flame atomic spectroscopy. The alkaline N was determined using the alkaline solution diffusion method. Briefly, 2 g of

biochar was weighed into the outer chamber of a diffusion dish, and 2 mL of boric acid indicator was added into the inner chamber of the dish. The dish was covered with a frosted glass and held using glycerin. Two mL of 1 mol L^{-1} NaOH was added to the outer chamber through the frosted glass gap and immediately covered tightly and held in place with rubber bands. The dish was incubated at 40 ℃ for 24 h and thereafter the solution in the inner chamber was titrated with 0.005 mol·L^{-1} H_2SO_4. The titre value was used to estimate the alkaline N content.

The heavy metal concentration was determined by weighing 0.5 g of the biochar sample and adding it into 30 mL polytetrafluoroethylene crucible, and then 1 to 2 drops of ultrapure water were added. Five mL of HNO_3:$HClO_4$ (in a ratio of 1:1, by v:v) and 5 mL of HF were added and left to stand overnight. The samples were then heated for 1 h at 100 ℃ and then the temperature was raised to 250 ℃ until the samples were devoid of color. After cooling, the samples were filtered in a 25 mL volumetric flask with ultrapure water, and the heavy metal content (cadmium (Cd), lead (Pb), copper (Cu), zinc (Zn), and nickel (Ni)) was determined *via* inductively coupled plasma mass spectrometry (ICP-MS) (NexlON 300X, Perkin Elmer, Waltham, MA, USA).

Fourier transform infrared (FTIR) spectroscopy was performed to determine the functional groups on the biochar surface. The biochar sample and KBr were crushed together in a ratio of 1:100 in an agate mortar after drying overnight in an oven at 80 °C. The greyish mixture was pressed into a delicate transparent sheet and each FTIR spectra was obtained *via* laser scanning with an FTIR spectrometer (vertex 70, Bruker, Billerica, MA) using a resolution of 4 cm^{-1} at wavenumbers ranging between 500 cm^{-1} and 4000 cm^{-1}.

For the determination of the specific surface area and the pore size distribution of the biochar sample, 0.1 g of biochar was weighed and degassed for 10 h at 105 °C to remove the substances adsorbed by the surface of the biochar sample. A multipoint Brunauer - Emmet -Teller (BET) device (Trister II 3020, Micromeritics Instrument Corp., Shanghai, China) was used to measure the specific surface area. The sample interface was obtained by scanning biochar samples *via* an electron microscope (Nova^{TM} NanoSEM 230, FEI Company, Hillsboro, OR, USA).

Heavy metal adsorption

The heavy metal adsorption study was performed as described by Zou *et al*. (2018), and $Pb(NO_3)_2$ and $Cd(NO_3)_2$ were used to prepare two solutions that each had a mass concentration of 50 mg L^{-1}. The pH of the solution was adjusted to 5.5 using 0.1 mol L^{-1} HCl and 0.1 mol L^{-1} NaOH. For each solution, 30 mL was poured into a triangular flask, and 0.05 g of the biochar sample was weighed and added into the flask. The mixtures that contained the biochar and $Pb(NO_3)_2$ or $Cd(NO_3)_2$, were shaken at 150 r/min for 2 h at a constant temperature shaker of 25 °C. It was then filtered and the filtrate was analyzed *via* an atomic absorption spectrometer coupled to a mass spectrometer ((ICP-MS) (NexlON 300X, Perkin Elmer, Waltham, MA) to determine the concentration of Pb^{2+} and Cd^{2+} in the respective solutions, both before and after the adsorption reaction. The adsorption of these heavy metals by the biochar was calculated according to Eq. 3,

$$Qt = (Co\text{-}Ct)V/M \quad (3)$$

where Qt (mg g^{-1}) is the amount adsorbed by the biochar, Co (mg L^{-1}) is the initial mass concentration of the Pb^{2+} and Cd^{2+} solutions, Ct (mg L^{-1}) is the mass concentration of the Pb^{2+} and Cd^{2+} in the solution after 2 h of adsorption, V (mL) is the volume of the solution

L, and *M* (g) is the mass of the biochar.

Data processing and statistical analysis

All data obtained were subjected to analysis of variance (ANOVA) using SPSS (version 20.0, IBM, Armonk, NY) software. The means were separated using the least significant difference (LSD) at the 5% level of probability (p-value was less than 0.05). Omnic (version 8.0, ThermoFisher, Waltham, MA) software was used to analyze the FTIR spectra of the biochar samples, while Origin (version 9.0, Originlab Co., Wellesley, MA, USA) software was used to process the FTIR figures.

RESULTS AND DISCUSSION

Physicochemical Properties of the Biochar Samples

The results in Table 1 showed that biochar yield decreased as the temperature increased. The yield decreased by 26.7% when the carbonization temperature was increased from 400 °C to 700 °C. At the same carbonization temperatures, the total biochar yields gradually decreased as the holding time increased (as shown in Table 2). No statistical difference ($p<0.05$) was observed in the yield change with a 2.5 h to 3 h holding time among all temperatures, except at 700 °C, which led to a reduction in the total yield. The highest yield (30.9%) was observed at 400 °C with a 1.5 h holding time, while the lowest yield (16.0%) was observed at 700 °C with a 3 h holding time (Table 2). This indicated that a lower holding time at a lower temperature resulted in a higher yield. The decrease in total biochar yield as the pyrolysis temperature and holding time were increased could be attributed to the breakdown of the basic primary structure of the biochar during pyrolysis. A decrease in the total biochar yield as the temperature increased had also been reported in oak, pine, sugarcane, and peanut shell biochar (Zhang *et al.* 2015); spent mushroom substrates biochar (Sarfraz *et al.* 2019; Zhao *et al.* 2019); pig manure (Gasco *et al.* 2018); and straw and lignosulfonate (Zhang *et al.* 2015). Previous reports had also shown that feedstock was partially combusted at lower pyrolysis temperatures, which resulted in a higher yield; while a higher temperature resulted in the complete combustion of the biomass (Angin 2013; Ghanim *et al.* 2016) as well as increased gasification (Colantoni *et al.* 2016; Li and Chen 2018), which resulted in a decrease in the total yield.

Investigating the effects of the pyrolysis temperature on the properties of the biochar showed that all the biochar samples were alkaline under all tested conditions, regardless of pyrolysis temperature and holding time (Tables 1 and 2). The alkaline properties of biochar had been previously been established by Mechler *et al.* (2018). Although the pH increased as the pyrolysis temperature was increased, the trend for the change in pH with respect to the holding time showed an irregular pattern, as there was variation among the evaluated holding times. However, the highest pH value for each temperature variation was observed with a holding time of 3 h, with the exception of 400 °C, where the highest pH value (9.7) was observed with a holding time of 2.5 h (Table 2). The interactive effect of the temperature and holding time yielded pH values that ranged from 9.6 to 10.1. The highest pH value (10.1) was obtained at 700 °C with a holding time of 3 h. The biochar produced at a lower carbonization temperature had a lower pH, because at this temperature, there was major amount of moisture loss, in addition to little volatilization of the organic constituents. However, as the pyrolysis temperature increased, there was an increase in the number of organic components in the raw material that

volatilized as the proportion of the inorganic mineral component also increased, which resulted in a higher pH (Novak 2009). Similarly, a high pH at the peak pyrolysis temperature has been attributed to an increase in the ash content. The large number of cations, *e.g.*, calcium (Ca), magnesium (Mg), potassium (K), and sodium (Na), contained in the ash are directly correlated to the high biochar pH (Cao *et al.* 2009). This result showed that a higher pyrolysis temperature and maximum holding time (3 h) increased the pH of the biochar. Zhao *et al.* (2019) reported that the highest pH value among different spent mushroom substrates was obtained at a peak temperature of 700 °C. An increase in the biochar pH as the pyrolysis temperature was increased has been reported for crop residue-derived biochar (Keiluweit *et al.* 2010; Yuan *et al.* 2011; Mukherjee and Zimmerman 2013), sugarcane straw biochar (Melo *et al.* 2013), and poultry litter biochar (Song and Guo 2012). Therefore, the derived biochar can be used successfully as a soil amendment, especially for acidic soils, when produced under the aforementioned conditions (700 °C and a 3 h holding time).

The carbon content of the tobacco stem biomass was 312 g/kg (Table 3). However, as observed in Table 1, the carbon content of the biochar was enriched after pyrolysis, which ranged from 577 g kg^{-1} at a pyrolysis temperature of 400 °C up to 606 g kg^{-1} at a pyrolysis temperature of 600 °C, and subsequently decreased to 599 g kg^{-1} at a pyrolysis temperature of 700 °C. This occurs since pyrolysis is a process of carbon enrichment. Observations also showed that the maximum C content was obtained with a holding time of 2 h for the various temperatures evaluated (Table 2). The C content values obtained at a holding time of 2 h were 644.6 g kg^{-1}, 645.2 g/kg, 651.7 g kg^{-1}, and 647.8 g kg^{-1} for 400 °C, 500 °C, 600 °C, and 700 °C, respectively (as shown in Table 2). The maximum C content of the biochar (651.7 g kg^{-1}) was obtained at 600 °C. The C content values obtained for the biochar samples were in the range of values obtained for the bamboo biochar in the study by Chen *et al.* (2016), the various crop residues, *i.e.*, wheat straw, maize straw, rice straw and rice husk, in the study by Bian *et al.* (2016), and the biochar from other feedstocks in the study by Sun *et al.* (2014). At all tested pyrolysis temperatures, the C content increased at a holding time of 1.5 h to 2 h and decreased at a holding time of 3 h. This could be attributed to the fact that as the temperature increased and the biochar was held for an increased period of time, more organic matter was converted into ash and an amorphous form of carbon (CO_2). The initial increase in the C content of the biochar samples as the temperature increased indicated that the degree of carbonization of the tobacco stem increased, which subsequently stabilized at the peak temperature. A decrease in the total biochar C content at the peak temperature had been previously been reported and was attributed to the loss of C-containing compounds at a higher pyrolysis temperature (Bergeron *et al.* 2013; Han *et al.* 2016; Wang *et al.* 2016; Zhao *et al.* 2019). During pyrolysis, the C-H and C-O bonds found in the biomass are broken, and the hydrogen (H) and oxygen (O) previously bound to the carbon are lost, in the form of gas or steam, and consequently the C content is increased (Mašek *et al.* 2013). Therefore, a high carbonization temperature (600 °C) and a moderate holding time of 2 h are suitable for the production of biochar that has a high carbon output requirement. The high C content of this biochar sample made it useful for the C sequestration of excess carbon from the atmosphere.

The ash content of the biochar increased with as the temperature increased (Table 1).

Table 1. The Main Effect of Pyrolysis Temperature on the Biochar Properties

Temperature (°C)	Yield (%)	Carbon Content (g kg^{-1})	pH	Volatile Matter (%)	Ash (%)
400	29.3 ± 0.42a	577.4 ± 14.75c	9.7 ± 0.02c	39.9 ± 4.38a	21.9 ± 1.01c
500	25.9 ± 0.40b	605.8 ± 9.03a	9.7 ± 0.03c	38.7 ± 4.47a	23.4 ± 1.07c
600	24.2 ± 0.38c	606.2 ± 10.42a	9.9 ± 0.03b	26.6 ± 2.00b	28.0 ± 1.01b
700	21.4 ± 1.42d	598.9 ± 37.35b	10.0 ± 0.05a	24.0 ± 4.28b	32.1 ± 1.54a

The mean of three replicates (n=3) is followed by ± Standard Error (SE). Means with the same letter are statistically similar. Those with different letters are significantly different (p-value was less than 0.05).

Table 2. The Interaction Effect of Temperature and Holding Time on the Biochar Properties

Temperature (°C)	Time (h)	Yield (%)	C (g kg^{-1})	pH	Volatile matter (%)	Ash (%)
400	1.5	30.9 ± 1.07a	551.7 ± 12.28b	9.7 ± 1.07a	43.9 ± 5.01a	21.7 ± 1.07a
	2.0	29.6 ± 5.00b	644.6 ± 13.25a	9.7 ± 1.01a	42.1 ± 3.00a	21.9 ± 1.01a
	2.5	28.3 ± 3.07c	559.7 ± 13.25b	9.7 ± 0.91a	36.8 ± 2.01b	22.0 ± 2.07a
	3.0	28.3 ± 2.07c	553.5 ± 20.25b	9.6 ± 0.81a	36.8 ± 1.01b	22.3 ± 2.07a
500	1.5	27.6 ± 5.00a	580.8 ± 18.00c	9.6 ± 1.01b	43.0 ± 2.01a	22.6 ± 1.02b
	2.0	25.8 ± 3.01b	645.2 ± 23.75a	9.7 ± 1.01a	42.0 ± 5.00a	22.9 ± 1.07ab
	2.5	25.2 ± 2.00b	598.4 ± 13.25b	9.6 ± 1.61b	35.2 ± 5.01b	23.5 ± 2.04ab
	3.0	25.1 ± 2.06b	598.7 ± 10.56b	9.8 ± 1.31a	34.8 ± 3.01b	24.8 ± 1.07a
600	1.5	25.6 ± 3.07a	598.7 ± 13.34b	9.9 ± 1.21a	33.2 ± 4.00a	27.0 ± 1.01b
	2.0	24.5 ± 1.10b	651.7 ± 20.08a	9.8 ± 1.02b	30.4 ± 3.31a	28.1 ± 2.04ab
	2.5	23.6 ± 2.06c	597.1 ± 18.14b	9.8 ± 1.07b	21.6 ± 5.32b	28.2 ± 1.07ab
	3.0	23.1 ± 3.01c	577.3 ± 14.23c	10.0 ± 2.04a	21.4 ± 4.21b	28.9 ± 1.07a
700	1.5	25.7 ± 1.04a	614.1 ± 18.46b	10.1 ± 1.12a	25.9 ± 3.58a	30.1 ± 1.12b
	2.0	24.0 ± 1.10b	647.8 ± 20.13a	9.8 ± 1.19b	24.6 ± 4.30a	30.3 ± 1.54b
	2.5	20.1 ± 2.01c	570.7 ± 18.14c	9.8 ± 1.13b	23.4 ± 3.89a	33.2 ± 1.54a
	3.0	16.0 ± 1.14d	560.6 ± 12.12d	10.1 ± 1.07a	22.5 ± 3.78a	34.9 ± 1.11a

The mean of three replicates (n=3) is followed by ± Standard Error (SE). Means with the same letter are statistically similar. Those with different letters are significantly different (p-value was less than 0.05).

Evaluating the effects of the total holding time on the ash content of the biochar samples showed that the ash content increased as the temperature and holding time increased, and was highest (34.9%) at a temperature of 700 °C and a holding time of 3 h (Table 2).

During the carbonization of the tobacco stem, a portion of the constituent internal mineral elements were converted into ash. A similar increase in the ash proportional content as the temperature increased had been reported in corn stalk and sawdust by Liu *et al.* (2014). Keiluweit *et al.* (2010) reported that biochar produced from herbaceous grasses had an ash content greater than 20% at a temperature of at least 400 °C and was statistically higher than the pine wood biochar (less than 4%). Ranges observed in this study were similar to those reported by Bian *et al.* (2016) for wheat straw, rice straw, maize straw, and rice husks. In addition, the total volatile matter (VM) content of the biochar decreased as the pyrolysis temperature was increased (Table 1). Similarly, it was observed that the VM content of the biochar decreased as the holding time increased. However, a slight increase in the VM content was observed at a pyrolysis temperature of 400 °C from 36.8% with a holding time of 2.5 h to 36.8% with a holding time of 3 h. The highest VM content (43.9%) was observed with a pyrolysis temperature of 400 °C and a holding time of 1.5 h, while the lowest VM content (21.4%) was obtained with a pyrolysis temperature of 600 °C and a holding time of 3 h (Table 2). A decrease in the VM content with an increase in the pyrolysis temperature had been previously documented by Li *et al.* (2018) for switchgrass, water oak, and biosolids. In addition, it was reported by Cantrell *et al.* (2012) that a greater amount of VM was removed while ash and fixed carbon were enriched at higher pyrolysis temperatures. The presence of cellulose and hemicellulose at lower temperatures had been linked to a higher amount of VM at lower temperatures (Jindo *et al.* 2014). At a pyrolysis temperature of 600 °C to 700 °C, there was no statistical difference in the VM content (as shown in Table 1), which indicated that most of the VM likely decomposed at a pyrolysis temperature of 600 °C. Consequently, no statistical decrease in the VM content was observed at pyrolysis temperatures greater than 600 °C (Li *et al.* 2018; Zhao *et al.* 2019).

The elemental composition of the biochar was influenced by both the temperature and the holding time (Tables 4 and 5). A pyrolysis temperature of 400 °C led to an N content (22.8 g kg^{-1}) that was higher than the feedstock N content (20.5 g kg^{-1}) (Tables 3 and 4). The values in Table 4 showed that the N content in the biochar decreased as the pyrolysis temperature increased. In addition, the alkaline N content increased as the pyrolysis temperature increased, although a slight decrease was observed at a pyrolysis temperature of 500 °C. However, there was an increasing trend for the alkaline N content as the total holding time was increased at a pyrolysis temperature of 500 °C and 600 °C, while it slightly decreased at a holding time of 3 h and a pyrolysis temperature of 400 °C (Table 5). The highest value of this fraction (51.1 mg/kg) was obtained at a pyrolysis temperature of 600 °C and a holding time of 3 h. However, variation in the holding time yielded an initial increase in the N content with a holding time of 1.5 h to 2 h, the N content value decreased with a holding time of 2.5 h, and, slightly increased with a holding time of 3h (Table 5). A maximum N content was observed with a holding time of 2 h across all tested pyrolysis temperatures. The highest N content (25.6 g kg^{-1}) was obtained with a pyrolysis temperature of 400 °C and a holding time of 2 h. Previous studies have shown that the N content of biochar decreases with an increase in carbonization temperature or time (Yin 2014), because the NH_4^+-N, NO_3-N, and N-containing volatile components in the biomass are lost at high temperatures (Xiao *et al.* 2018). Similar to the author's observations, Zhao *et al.* (2015) showed that when the pyrolysis temperature was increased

from 300 °C to 600 °C, the N content of the biochar, which was derived from apple twigs, first increased and then decreased, and obtained the highest N content value at a pyrolysis temperature of 400 °C.

As shown in Table 4, there was an increased amount of enrichment of the total P and K as the pyrolysis temperature increased, when compared to the total P and K content in the feedstock, 1.3 g kg^{-1} and 65.6 g kg^{-1}, respectively (Table 3). Similarly, the amount of effective P and K increased as the pyrolysis temperature increased (Table 4). An increase in P and K with an increase in pyrolysis temperature had been previously reported by Ahmad *et al.* (2017). The total P value increased by 59.6 % from an average of 2.2% at a pyrolysis temperature of 400 °C to an average of 5.47% at a pyrolysis temperature of 700 °C. The data in Table 5 showed that the P-value increased consistently as the holding time increased from 1.5 h to 3 h across all tested pyrolytic temperatures. However, an irregular pattern emerged for the amount of effective P at a pyrolysis temperature of 500 °C and 700 °C. The highest P concentration (7.82 g kg^{-1}) was obtained with a pyrolysis temperature of 600 °C and a holding time of 3 h. The amount of effective P was observed to follow a similar trend to the total P content in terms of the temperature and holding time, although its highest value was obtained with a pyrolysis temperature of 700 °C and a holding time of 3 h. The total potassium content of the biochar increased as the temperature increased from 400 °C to 600 °C and then decreased at a pyrolysis temperature of 700 °C (Table 4). In addition, Table 4 showed an increase in the K content as the holding time increased from 500 °C and 600 °C. However, at a pyrolysis temperature of 400 °C, there was a slight decrease in the K content at a holding time of 2.5 h (117.5 g kg^{-1}) from a holding time of 2 h (119.3 g kg^{-1}). This was also observed at a pyrolysis temperature of 700 °C, where the K content values decreased from 134.9 g/kg at a holding time of 2.5 h to 131.5 g kg^{-1} at a holding time of 3 h. The highest K content (167.8 g kg^{-1}) was observed with a pyrolysis temperature of 600 °C and a holding time of 3 h (as shown in Table 5). The K content values of the tobacco stem biochar samples ranged from 88.4 g kg^{-1} to 167.8 g kg^{-1}. Previous studies had reported a wide range of N, P, and K concentrations in biochars, although plant-derived biochars contained a relatively lower amount of nutrient elements than those derived from manure and food wastes (Cantrell *et al.* 2012). In a meta-analysis by Chan and Xu (2009), the reported concentrations of total N contents that ranged from 1.8 g kg^{-1} to 56.4 g kg^{-1}, total P contents that ranged from 2.7 g kg^{-1} to 480 g kg^{-1}, and total K contents that ranged from 1.0 g kg^{-1} to 58 g kg^{-1}. In addition, a wide range of values had been obtained in various crop residues. The total N content ranged from 4.3 g kg^{-1} (coconut shell biochar) to 47.8 g kg^{-1} (cotton stalk biochar). The total P content of the various biochars ranged from less than 0.1 g kg^{-1} for palm shell and coconut shell biochars to 4.2 g kg^{-1} for olive pomace biochar, while the total K content ranged from 0.6 g/kg for palm shell biochar to 60 g/kg for wheat straw biochar (Windeatt *et al.* 2014). In crop residue biochars (wheat straw, rice straw, maize straw, and rice husk), the N content ranged from 8.47 g kg^{-1} to 16.1 g kg^{-1}, the P content ranged from 1.67 g kg^{-1} to 4.43 g kg^{-1}, and the K content ranged from 12.9 g kg^{-1} to 32.0 g kg^{-1} (Bian *et al.* 2016). Similar ranges had been reported in spent mushroom substrate biochars (Sarfraz *et al.* 2019; Zhao *et al.* 2019). A meta-analysis by Ippolito *et al.* (2015) reported an average total concentration of 0.9 g kg^{-1} to 32.8 g kg^{-1} for N, an average total concentration of 0.32 g kg^{-1} to 60.8 g kg^{-1} for P, and an average total concentration of 0.7 g kg^{-1} to 116 g kg^{-1} for K, for a wide range of biochar materials. The range of the values obtained from this study showed that the total N, P, and K content values found in the tobacco stem biochar were, on average, higher than most ranges reported in other studies. This indicated that the tobacco plant took up higher

nutrients from the soil. Therefore, this biochar will be useful as a fertilizer either by itself or as part of a biochar compound fertilizer, which can be re-applied into the soil after harvest to return back most of the soil nutrients taken up, so to maximize its benefit.

Table 3. Elemental Composition in the Tobacco Stem Feedstock

Sample	C Content (g kg^{-1})	N Content (g kg^{-1})	P Content (g kg^{-1})	K Content (g kg^{-1})
Tobacco Stem	312.3	20.5	1.3	65.6

Table 4. The Main Effect of Pyrolysis Temperature on the Elemental Composition in the Biochar Samples

Temperature (°C)	N (g kg^{-1})	P (g kg^{-1})	K (g kg^{-1})	Available Phosphorus (mg kg^{-1})	Alkaline Nitrogen (mg kg^{-1})	Available Potassium (mg kg^{-1})
400	22.8 ± 0.64a	2.2 ± 0.02c	112.4 ± 5.43c	12.9 ± 1.05d	46.1 ± 2.54b	54.7 ± 2.13c
500	20.1 ± 0.45b	3.0 ± 0.03b	124.4 ± 8.41b	17.6 ± 2.03c	45.1 ± 2.28b	56.5 ± 1.45b
600	18.8 ± 0.48c	5.4 ± 0.08a	161.1 ± 13.30a	19.2 ± 1.05b	47.5 ± 1.67a	56.9 ± 1.79b
700	16.5 ± 0.74d	5.5 ± 0.12a	126.2 ± 3.36b	27.7 ± 1.06a	48.8 ± 1.50a	62.5 ± 2.14a

The mean of three replicates (n=3) is followed by ± Standard Error (SE). Means with the same letter are statistically similar. Those with different letters are significantly different (p-value was less than 0.05)

Investigating the effects of the pyrolysis temperature on the heavy metal content indicated that the concentrations of Ni and Cd in the biochar increased after the biomass underwent pyrolysis (Table 7). The amount of Ni and Cd found in tobacco stems was lower in comparison to the other heavy metals found (Table 6). However, the amount of Zn found in the biochar was reduced after undergoing pyrolysis, and the amount of Cu decreased at all pyrolysis temperatures, excluding a pyrolysis temperature of 700 °C, in which the amount of Cu increased. An irregular trend occurred for the Pb concentration as the pyrolysis temperature increased. The highest heavy metal concentrations were observed at the peak temperature (700 °C), except for Cd, which was highest at a pyrolysis temperature 400 °C. The effects of the holding time on the heavy metals concentration in the biochar were shown in Table 8, and the Ni concentration ranged from 1.4 mg kg^{-1} at a pyrolysis temperature of 400 °C and a holding time of 1.5 h to 13.3 mg kg^{-1} at a pyrolysis temperature of 500 °C and a holding time of 2 h. The Cu concentration ranged from 4.4 mg kg^{-1} at a pyrolysis temperature of 400 °C and a holding time of 1.5 h to 20.9 mg kg^{-1} at a pyrolysis temperature of 500 °C and a holding time of 2 h. The concentration values for Zn ranged from 14.5 mg kg^{-1} at a pyrolysis temperature of 600 °C and a holding time of 3 h to 104.4 mg kg^{-1} at a pyrolysis temperature of 700 °C and a holding time of 2 h.

Table 5. The Interaction Effect of Temperature and Holding Time on the Elemental Composition in the Biochar Samples

Temperature (°C)	Time (h)	N (g kg^{-1})	P (g kg^{-1})	K (g kg^{-1})	Effective Phosphorus (mg kg^{-1})	Alkaline Nitrogen (mg kg^{-1})	Effective Potassium (mg kg^{-1})
400	1.5	21.8 ± 0.03c	1.7 ± 0.01b	88.4 ± 7.15c	11.0 ± 0.35c	39.1 ± 0.07b	49.1 ± 2.16b
	2.0	25.6 ± 0.03a	2.1 ± 0.11b	119.3 ± 7.25b	12.9 ± 0.26b	47.8 ± 1.88a	52.3 ± 1.19b
	2.5	21.4 ± 0.03c	2.4 ± 0.01a	117.5 ± 7.56b	13.5 ± 0.75b	48.7 ± 1.12a	58.2 ± 1.18a
	3.0	22.9 ± 0.03b	2.6 ± 0.25a	124.5 ± 3.89a	14.1 ± 0.91a	48.7 ± 3.15a	59.3 ± 2.19a
500	1.5	19.2 ± 0.03c	2.5 ± 0.01b	109.1 ± 7.12d	17.1 ± 1.25a	41.4 ± 0.74b	50.3 ± 1.20c
	2.0	22.1 ± 0.03a	2.5 ± 0.11b	118.8 ± 7.06c	17.1 ± 1.33a	44.6 ± 0.81b	53.2 ± 1.21c
	2.5	19.3 ± 0.03c	3.5 ± 0.32a	124.5 ± 1.89b	17.9 ± 1.03a	48.0 ± 0.04a	59.3 ± 2.32b
	3.0	19.9 ± 0.03b	3.6 ± 1.25a	145.2 ± 7.03a	18.3 ± 1.06a	46.4 ± 0.63a	63.2 ± 1.23a
600	1.5	18.7 ± 0.03b	2.9 ± 0.13d	157.7 ± 1.37b	17.1 ± 1.06a	45.5 ± 1.36c	51.2 ± 2.24c
	2.0	20.8 ± 0.03a	4.4 ± 0.24c	157.8 ± 1.45b	19.1 ± 1.07a	46.1 ± 0.73b	52.7 ± 5.25c
	2.5	17.4 ± 0.03c	6.6 ± 0.07b	161.4 ± 3.05a	20.0 ± 2.14a	47.5 ± 1.64b	59.6 ± 3.27b
	3.0	18.3 ± 0.03b	7.8 ± 0.37a	167.8 ± 2.97a	20.5 ± 2.05a	51.1 ± 0.69a	64.1 ± 5.47a
700	1.5	15.4 ± 0.03b	3.3 ± 0.13d	112.1 ± 3.38c	26.7 ± 1.02a	43.8 ± 0.21c	58.7 ± 2.28b
	2.0	19.8 ± 0.03a	4.2 ± 0.23c	126.5 ± 7.12b	27.9 ± 2.11a	47.8 ± 1.05b	59.5 ± 2.79b
	2.5	15.1 ± 0.03b	6.9 ± 0.23b	134.9 ± 1.09a	27.3 ± 1.05a	48.3 ± 4.10b	65.3 ± 2.70a
	3.0	15.8 ± 0.03b	7.6 ± 0.15a	131.5 ± 1.36a	28.9 ± 1.20a	50.1 ± 3.66a	66.4 ± 3.31a

The mean of three replicates (n=3) is followed by ± Standard Error (SE). Means with the same letter are statistically similar. Those with different letters are significantly different (p-value was less than 0.05)

Table 6. The Heavy Metal Concentrations in the Tobacco Stems

Sample	Ni (mg kg^{-1})	Cu (mg kg^{-1})	Zn (mg kg^{-1})	Cd (mg kg^{-1})	Pb (mg kg^{-1})
Tobacco Stem	2.3	15.1	81.0	0.6	4.2

The Cd concentration ranged from 0.2 mg kg^{-1} at a pyrolysis temperature of 500 °C and a holding time of 1.5 h to 1.7 mg kg^{-1} at a pyrolysis temperature of 600 °C and a holding time of 3 h. In addition, the Pb concentration ranged from 1.1 mg kg^{-1} at a pyrolysis temperature of 500 °C and a holding time of 1.5 h to 7.9 mg kg^{-1} at a pyrolysis temperature of 500 °C and a holding time of 2.5 h.

Table 7. The Main Effect of Pyrolysis Temperature on the Concentrations of Heavy Metals in the Biochar Samples

Temperature (°C)	Ni (mg kg^{-1})	Cu (mg kg^{-1})	Zn (mg kg^{-1})	Cd (mg kg^{-1})	Pb (mg kg^{-1})
400	4.6 ± 0.73d	9.5 ± 1.60d	47.8 ± 10.44c	0.9 ± 0.13a	3.2 ± 0.70c
500	7.7 ± 1.46b	13.4 ± 2.67b	56.3 ± 9.24b	0.7 ± 0.11b	5.2 ± 0.95a
600	6.6 ± 0.52c	11.3 ± 1.65c	48.3 ± 10.92c	0.8 ± 0.21b	4.4 ± 0.44b
700	8.3 ± 0.88a	15.6 ± 4.04a	78.4 ± 5.27a	0.5 ± 0.08c	5.3 ± 0.33a

The mean of three replicates (n=3) is followed by ± Standard Error (SE). Means with the same letter are statistically similar. Those with different letters are significantly different (p-value was less than 0.05)

Table 8. The Interaction Effect of Temperature and Holding time on the Concentrations of Heavy Metals in the Biochar Samples

Temper-ature (°C)	Time (h)	Ni (mg kg^{-1})	Cu (mg kg^{-1})	Zn (mg kg^{-1})	Cd (mg kg^{-1})	Pb (mg kg^{-1})
400	1.5	1.4 ± 0.33c	4.4 ± 0.54d	24.7 ± 6.35c	0.3 ± 1.37d	1.3 ± 0.60a
	2	6.7 ± 2.75a	6.7 ± 2.05c	16.5 ± 7.41d	0.8 ± 0.02c	1.4 ± 0.98a
	2.5	5.4 ± 0.78b	17.2 ± 0.78a	80.3 ± 4.36a	1.4 ± 0.07a	5.6 ± 1.67a
	3	5.0 ± 1.45b	10.2 ± 1.45b	70.3 ± 6.27b	1.0 ± 0.02b	4.6 ± 0.77b
500	1.5	3.3 ± 1.55c	4.5 ± 0.15c	18.5 ± 3.79a	0.2 ± 0.06c	1.1 ± 1.45d
	2	13.3 ± 7.53a	13.3 ± 1.48b	54.8 ± 8.55c	0.8 ± 0.02b	5.4 ± 1.27c
	2.5	7.4 ± 0.91b	20.9 ± 2.44a	85.1 ± 6.52a	1.0 ± 0.03a	7.9 ± 2.33a
	3	6.4 ± 0.91b	15.1 ± 1.09b	65.1 ± 5.85b	0.8 ± 0.04b	6.7 ± 1.9b
600	1.5	4.8 ± 1.32c	16.0 ± 2.86b	80.8 ± 1.63a	0.3 ± 0.01c	5.9 ± 0.60a
	2	7.9 ± 0.79a	16.3 ± 1.72a	72.7 ± 2.67b	0.3 ± 0.05c	5.2 ± 0.06b
	2.5	5.9 ± 1.57b	5.9 ± 1.19d	24.5 ± 3.74c	0.7 ± 0.07b	3.2 ± 0.04c
	3	7.9 ± 0.96a	6.9 ± 0.94c	14.5 ± 3.81d	1.7 ± 0.05a	3.2 ± 1.60d
700	1.5	5.9 ± 0.84c	15.4 ± 1.93b	70.4 ± 7.06b	0.3 ± 0.05b	6.5 ± 1.58a
	2	12.3 ± 0.53a	17.4 ± 1.80a	104.4 ± 4.93a	0.5 ± 0.02b	5.3 ± 1.29b
	2.5	8.5 ± 0.75b	16.3 ± 0.81ab	76.4 ± 12.09b	0.5 ± 0.04c	4.0 ± 0.11c
	3	6.5 ± 0.91c	14.4 ± 0.25b	66.4 ± 9.90b	0.8 ± 0.06a	5.0 ± 0.16b

The mean of three replicates (n=3) is followed by ± Standard Error (SE). Means with same letter are statistically similar. Those with different letters are significantly different (p-value was less than 0.05)

The European Biochar Foundation (EBF) (2017) stated a safe range for the following heavy metal concentrations in biochar: the Pb concentration should be less than 150 mg kg^{-1}; the Cd concentration should be less than 1.5 mg kg^{-1}; the Cu concentration should be less than 100 mg kg^{-1}; the Ni concentration should be less than 50 mg kg^{-1}; and the Zn concentration should be less than 400 mg kg^{-1}. According to the values given above, the Cd concentration (1.71 mg/kg) at a pyrolysis temperature of 600 °C and a holding time of 3 h was higher than the given threshold (less than 1.5 mg kg^{-1}). However, the other

heavy metal concentrations were well below the thresholds required for the safe usage of the biochar in the environment, and therefore, could be applied to the soil without environmental concerns. Previous studies have shown that the concentration of heavy metals can be greater in the biochar than in the feedstock (Sarfraz *et al.* 2019; Zhao *et al.* 2019). However, biochar is able to effectively bind and immobilize heavy metals for a long period of time, but the length of time is yet to be determined (EBF 2017). Since the amount of biochar used for agricultural purposes is relatively low, any toxic accumulation could be ruled out, particularly when the concentration thresholds are slightly higher than stated by the EBF.

Microstructure and Surface Properties of the Biochar Samples

The surface morphology of the biochar samples at 400 ℃, 500 ℃, 600 ℃, and 700 ℃ (all at a holding time of 2 h) were determined *via* scanning electron microscopy (SEM) images, which indicated their porous structure (as shown in Fig. 6a through Fig. 6d). Uzun *et al.* (2010) reported that during pyrolysis, the porosity of the feedstock increased, due to the discharge of the volatile compounds and the chemical reactions that occurred between the volatile compounds, minerals, and inorganic compounds present in the feedstock, which was similar to the observations the authors noticed in the SEM images. At higher temperatures (600 ℃ and 700 ℃), there was an increase in the surface area of the biochar samples. An increased surface area implied a greater number of porous structures within the biochar (Inyang *et al.* 2010; Kloss *et al.* 2014).

The pores found in the biochar samples could be divided into micropores (less than 0.8 nm), small pores (0.8 nm to 2 nm), mesopores (2 nm to 50 nm), and macropores (greater than 50 nm) (Chia *et al.* 2015). The range of values obtained showed that all the pores found in the biochar samples were mesopores (Fig. 1b). The surface area increased as the pyrolysis temperature increased from 400 ℃ to 700 ℃ (Fig. 1a), while the average pore diameter decreased as the pyrolysis temperature increased (as shown in Fig. 1b). However, when the holding time was varied, the biochar samples produced with a holding time of 1.5 h had macropores at all tested temperatures, *i.e.*, 400 °C (53.5 Å), 500 °C (52.5 Å), and 600 °C (52.5 Å). The improved porosity of the biochar samples had been reported by Joseph *et al.* (2010) to play an important role in soil aeration and moisture retention when applied as a soil amendment. However, after pyrolysis, there was a decrease in the pore diameter of the biochar samples as the temperature increased (as shown in Fig. 1b). In addition, the effects of variation in the total holding time on the pore diameter were shown in Table 9. Consequently, the surface and micropore areas of the biochar samples increased as the temperature and holding time increased (Fig. 1 and Table 9). The highest surface area of the biochar samples (50.6 m^2 g^{-1}) and micropore areas (57.1 m^2 g^{-1}) were obtained with a pyrolysis temperature of 700 °C and a holding time of 3 h. The decrease in the average pore size of the biochar samples as the temperature increased could be attributed to the gradual development of mesopores on the surface of the biochar samples and the appearance of micropores, or the smaller pores becoming clogged. An increase in the surface area and micropore diameter as the pyrolysis temperature increased had been previously reported for rice husk and cotton straw biochar (Jia *et al.* 2018), crop residues (Bian *et al.* 2016), and hardwood (Sun *et al.* 2014; Domingues *et al.* 2017). Surface area is a key factor that regulates the ability of a material to adsorb chemical compounds, and a larger surface area implies a greater number of porous structures within the biochar (Inyang *et al.* 2010; Kloss *et al.* 2014). The application of the experimental biochar to soil could enhance its interaction with the plant roots, soil microorganisms, and minerals to promote

soil properties, therefore improving the soil and plant productivity (Joseph *et al.* 2010; Liu *et al.* 2013). The tobacco biochar produced with a pyrolysis temperature of 700 °C and a holding time of 3 h would be ideal for nutrient retention as a slow-release fertilizer and could be useful for adsorption of contaminants in soil or water.

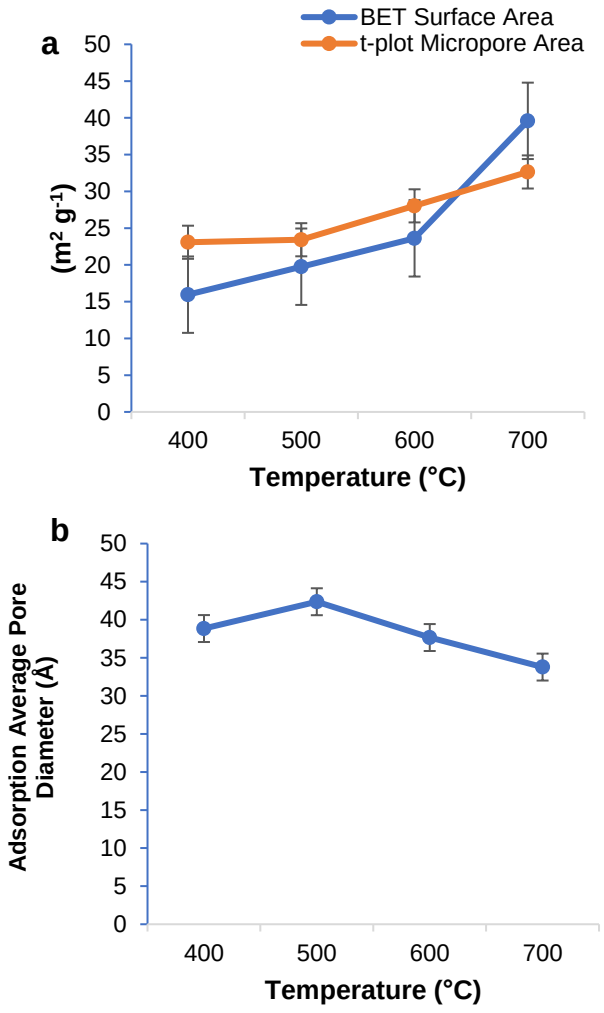

Fig. 1. Main effect of pyrolysis temperature on the BET surface area and porosity of the biochar samples. Error bars indicate standard error of the mean (n=3)

Fourier Transform Infrared Spectrometry Analysis of the Biochar Samples

Figures 2 through 5 show the FTIR peaks appearing from 400 cm^{-1} to 4000 cm^{-1} and showed the change in the chemical bonds as the pyrolysis temperature was increased with various holding times. The weak O-H group present in all of the biochar samples that was found between 3400 cm^{-1} and 3700 cm^{-1} could be the result of acid and/or alcohol structures (Wu *et al.* 2012). The adsorption peaks that represented the C=O and C=C stretching, and the aromatic C-H appeared between 1400 cm^{-1} and 1600 cm^{-1}. The aromatic structures (C=C) found in the FTIR spectra at holding times of 1.5 h and 3 h and the C-H bonds found in all the holding times were gradually lost as the pyrolysis temperature increased from 400 °C to 700 °C.

Table 9. Interaction Effect of Temperature and Holding Time on the BET Surface Area and Porosity of the Biochar Samples

Temperature (°C)	Time (h)	BET Surface Area (m^2 g^{-1})	t-plot Micropore Area (m^2 g^{-1})	Adsorption Average Pore Diameter (Å)
400	1.5	10.5 ± 0.38d	6.6 ± 0.05d	53.5 ± 0.94a
	2	14.5 ± 0.60c	11.7 ± 0.28c	37.4 ± 0.51b
	2.5	18.8 ± 0.77b	29.5 ± 0.50b	35.6 ± 0.60b
	3	20.1 ± 0.86a	45.0 ± 0.26a	30.4 ± 1.19c
500	1.5	12.7 ± 0.12c	6.9 ± 0.09d	52.5 ± 0.92a
	2	11.9 ± 0.14c	16.3 ± 0.70c	46.7 ± 1.00a
	2.5	20.1 ± 1.56b	19.8 ± 0.93b	40.0 ± 0.72b
	3	34.3 ± 0.45a	50.5 ± 1.31a	30.4 ± 1.10c
600	1.5	14.7 ± 0.68c	7.9 ± 0.11d	52.5 ± 0.78a
	2	16.5 ± 0.99c	20.0 ± 0.70c	35.8 ± 0.21b
	2.5	25.7 ± 0.68b	30.0 ± 0.89b	38.7 ± 1.46b
	3	37.5 ± 0.94a	55.0 ± 0.94a	25.9 ± 1.26c
700	1.5	30.0 ± 0.69c	15.4 ± 0.77d	37.1 ± 0.70a
	2	40.7 ± 1.24b	25.0 ± 0.33c	35.1 ± 0.74a
	2.5	39.4 ± 0.86b	34.6 ± 0.72b	36.0 ± 0.75a
	3	50.6 ± 1.90a	57.1 ± 0.20a	25.6 ± 0.36b

The mean of three replicates (n=3) is followed by ± Standard Error (SE). Means with the same letter are statistically similar. Those with different letters are significantly different ($p < 0.05$).

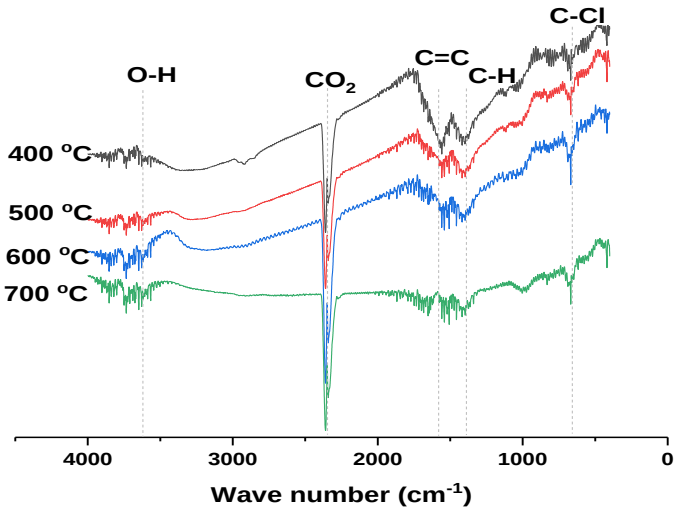

Fig. 2. FTIR spectra of biochar samples retained for 1.5 h at different temperatures

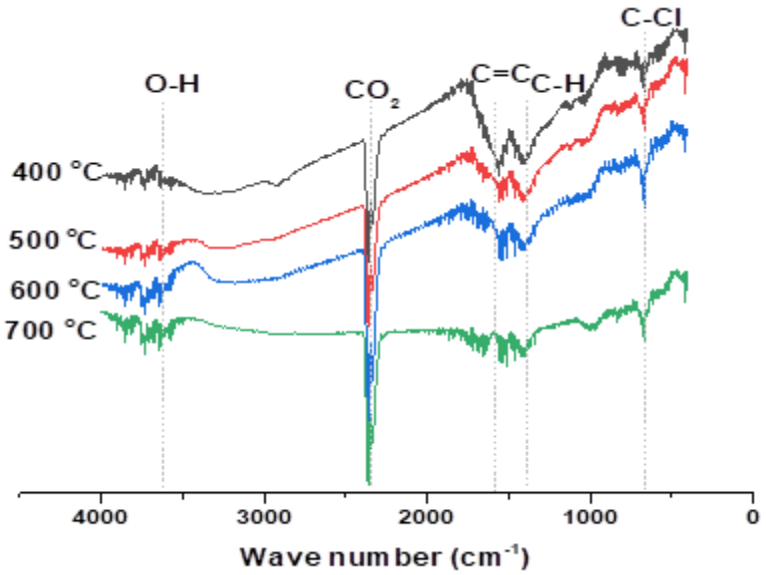

Fig. 3. FTIR spectra of biochar samples retained for 2 h at different temperatures

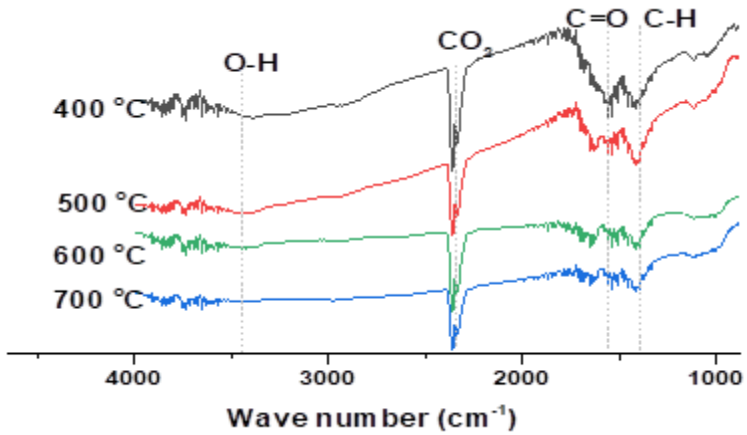

Fig. 4. FTIR spectra of biochar samples retained for 2.5 h at different temperatures

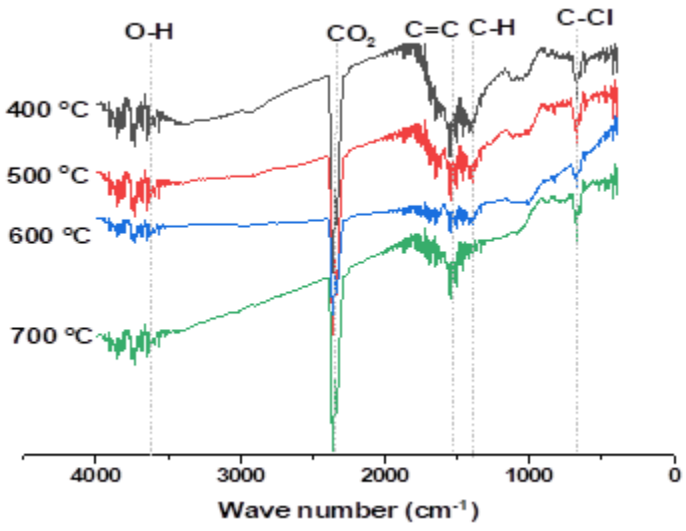

Fig. 5. FTIR spectra of biochar samples retained for 3 h at different temperatures

The disappearance of these functional groups at higher temperatures resulted in an increased mass loss and thus, a reduced biochar yield (Zhao *et al.* 2019). The weakening of the peaks as the pyrolysis temperature increased had been previously reported by Jin *et al.* (2016). The CO_2 peak was present with a high intensity for all the biochar samples, regardless of temperature and holding time. The aliphatic and aromatic C compounds observed in the biochar samples signified their high C content. Adsorption peaks that represent various functional groups are often observed in biochar (Domingues *et al.* 2017). The presence of reactive O-containing functional groups on the surface of the biochar samples, as well as carboxylic or hydroxylic groups, showed its ability to interact with polar organic compounds (Brodowsky *et al.* 2005). Generally, the cation exchange capacity of the soil amended with biochar can be improved, due to the presence of oxidized functional groups on the surface of the biochar (Liang *et al.* 2006). Therefore, the tobacco stem biochar samples with oxygen functional groups could be suitable for soil amendment, in order to improve the physical property and chemical properties of the soil.

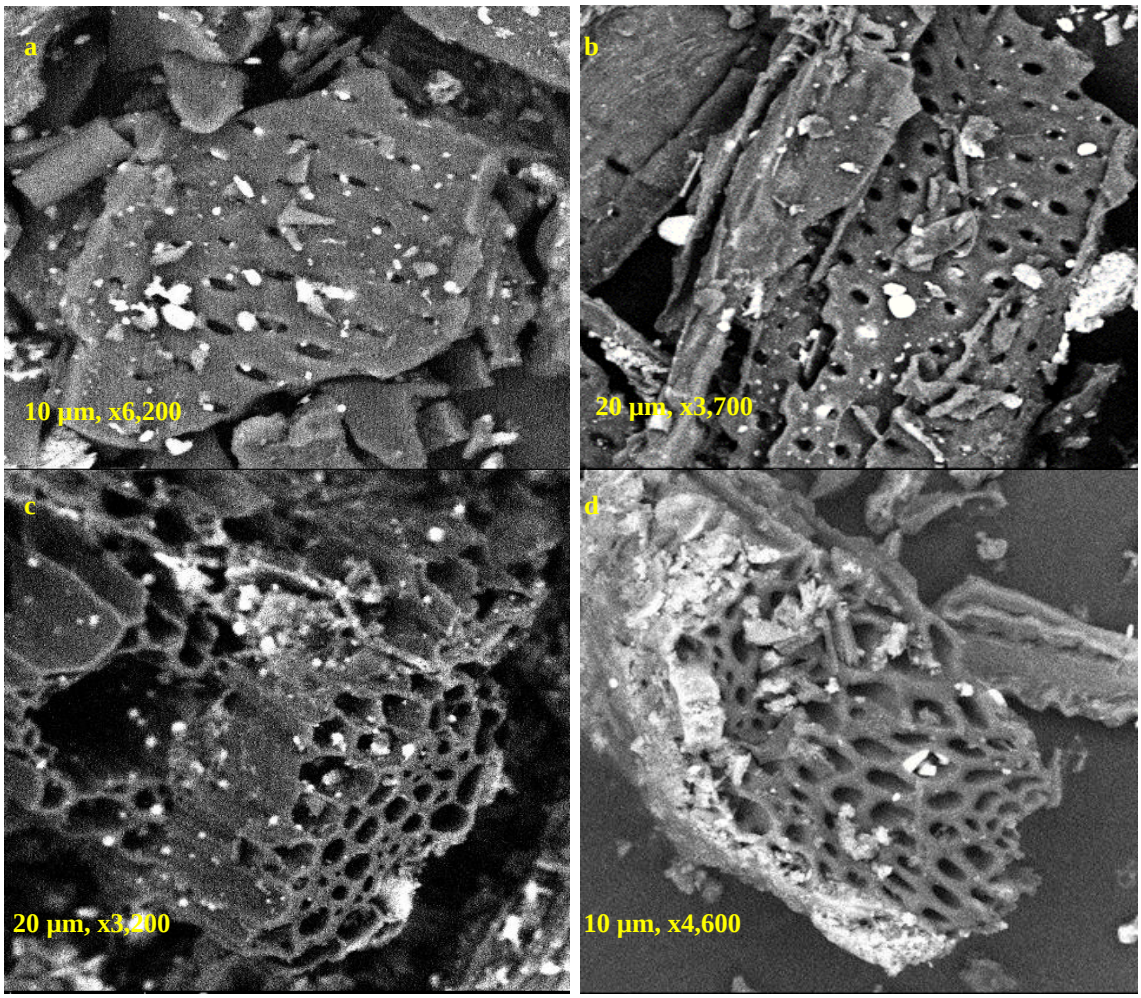

Fig. 6. SEM images of biochar samples at (a) 400 °C (b) 500 °C (c) 600 °C (d) 700 °C held for 2 h

The Adsorption of Pb^{2+} and Cd^{2+} by Tobacco Stem Biochar

Table 10 showed that the adsorption amount for Pb^{2+} and Cd^{2+} increased as the pyrolysis temperature was increased. The maximum adsorption amount was obtained with

a pyrolysis temperature of 700 °C for both metals. Table 11 shows that the amount of Pb^{2+} and Cd^{2+} adsorbed by the tobacco biochar increased as the temperature and holding time increased, with a pyrolysis temperature of 700 °C and a holding time of 3 h having the greatest adsorption value for Pb^{2+} (22.3 $mg \cdot g^{-1}$) and for Cd^{2+} (19.2 $mg \cdot g^{-1}$), which was equivalent to 44.5% and 38.3%, respectively. The amounts of Pb^{2+} and Cd^{2+} adsorbed by the biochar samples were shown to increase when the pyrolysis temperature was increased (Wang *et al.* 2014b; Zhu *et al.* 2016; Zhu *et al*. 2017; Jia *et al.* 2018). The amount of Pb^{2+} adsorbed ranged from 11.9 $mg \cdot g^{-1}$ to 22.3 $mg \cdot g^{-1}$, while the amount of Cd^{2+} adsorbed ranged from 12.1 $mg \cdot g^{-1}$ to 19.2 $mg \cdot g^{-1}$. A higher adsorption value was observed for Pb^{2+} over Cd^{2+}. This could be connected to a higher affinity for Pb^{2+}, since the biochar had a lower concentration of Pb^{2+} when compared to Cd^{2+} (Table 8).

Table 10. The Main Effect of Pyrolysis Temperature on the Amount of Pb^{2+} and Cd^{2+} Adsorbed by the Biochar Samples

Temperature (°C)	Adsorption of Pb^{2+} (mg x g^{-1})	Adsorption of Cd^{2+} (mg x g^{-1})
400	13.4 ± 0.43d	13.2 ± 0.41d
500	15.9 ± 0.51c	14.7 ± 0.45c
600	19.1 ± 0.53b	16.1 ± 0.48b
700	20.2 ± 0.49a	17.3 ± 0.51a
The mean of three replicates (n=3) is followed by ± Standard Error (SE). Means with the same letter are statistically similar. Those with different letters are significantly different (p-value was less than 0.05)		

Table 11. Interaction Effect of Pyrolysis Temperature and Holding Time on Biochar Adsorption of Pb^{2+} and Cd^{2+}

Temperature (°C)	Time(h)	Adsorption of Pb^{2+} (mg x g^{-1})	Adsorption of Cd^{2+} (mg x g^{-1})
400	1.5	11.9 ± 0.09d	12.1 ± 0.39c
	2	12.9 ± 0.36c	12.7 ± 0.13bc
	2.5	13.8 ± 0.39b	13.3 ± 0.20b
	3	14.9 ± 0.25a	14.9 ± 0.00a
500	1.5	14.4 ± 0.32d	13.21 ± 0.03c
	2	15.0 ± 0.01c	14.6 ± 0.43b
	2.5	16.1 ± 0.15b	14.4 ± 0.38b
	3	17.9 ± 0.01a	16.4 ± 0.44a
600	1.5	17.6 ± 1.40b	14.5 ± 0.34c
	2	18.7 ± 0.18ab	16.3 ± 0.18b
	2.5	19.1 ± 0.47ab	15.7 ± 0.42b
	3	21.2 ± 0.34a	18.0 ± 0.05a
700	1.5	19.1 ± 0.01c	15.8 ± 0.52c
	2	19.1 ± 0.01c	17.9 ± 0.08c
	2.5	20.5 ± 0.21b	16.4 ± 0.43b
	3	22.3 ± 0.28a	19.2 ± 0.47a
The mean of three replicates (n=3) is followed by ± Standard Error (SE). Means with the same letter are statistically similar. Those with different letters are significantly different (p-value was less than 0.05)			

The presence of inorganic salts, *e.g.*, CO_3^{2-}, SiO_3^{2-}, and PO_4^{3-}, in the biochar could be connected to its higher pH, which could in turn form precipitates with the metals, which would reduce their solubility by adsorbing them into the surface of the biochar. In addition, the increase in the amount of adsorption as the temperature increased could be attributed to the increase in surface area at higher pyrolysis temperatures (as shown in Table 9). The adsorption performance of biochar has been linked with the chemical groups found on the biochar surface (Sardella *et al.* 2015) as well as the surface area (Tekin *et al.* 2016). The biochar sample derived from maize straw that had the highest porosity was reported by Zhang *et al.* (2018) had the highest Pb^{2+} adsorption value (98.3%) when compared to the sunflower and wheat straw biochars. However, the maximum adsorption values obtained in this study (44.5% for Pb^{2+} and 38.3% for Cd^{2+}) were lower than the reported values for Pb^{2+} by Li *et al.* (2014) and Zhang *et al*. (2018) and the reported values for Pb^{2+} and Cd^{2+} by Li *et al.* (2015) and Jia *et al.* (2018). However, the biochar could be useful for heavy metal sorption in its present form or modified/engineered to improve its effectiveness.

CONCLUSIONS

1. The total biochar yield decreased as the temperature and holding time increased. The lowest yield (16.0%) was obtained with a pyrolysis temperature of 700 °C and a holding time of 3 h, whereas the highest yield (30.9%) was obtained with a pyrolysis temperature of 400 °C and a holding time of 1.5 h.
2. The derived biochar was alkaline and had a pH range of 9.6 to 10.1. The highest pH was obtained with a pyrolysis temperature of 700 °C and a holding time of 3 h. This made the biochar produced at this temperature suitable as a soil amendment for acidic soils.
3. The peak C content (651.7 g/kg) was recorded at a pyrolysis temperature of 600 °C and a holding time of 2 h. The high C content of the biochar showed that it could be useful for carbon sequestration. The amount of ash increased as the temperature and holding time increased, while the amount of VM decreased as the temperature and holding time increased. The highest content values that were obtained for N, P, and K were 25.6 g/kg (a pyrolysis temperature of 400 °C and a holding time of 2 h), 7.8 g/kg (a pyrolysis temperature of 600 °C and a holding time of 3 h), and 167.8 g/kg (a pyrolysis temperature of 600 °C and a holding time of 3 h), respectively. Since the levels of nutrient elements found in the biochar were greater than several types of other crop residue biochars, this meant it could be useful as a fertilizer or as a biochar compound fertilizer especially on the same soil after harvest since the crop apparently took up high soil nutrients into the plant biomass.
4. The heavy metal content in the biochar was noticeably lower than the threshold for heavy metals in biochar. Therefore, the biochar could be used safely in the environment.
5. The biochar surface had mesopores, and the highest surface and micropore areas (50.6 $m^2\ g^{-1}$ and 57.1 $m^2\ g^{-1}$, respectively) were obtained from biochar produced with a pyrolysis temperature of 700 °C and a holding time of 3 h. This property made it useful in terms of sorption of contaminants in the environment. A wide range of aliphatic and aromatic C functional groups were found on the biochar surface, which indicated its high C content. All the biochar samples evaluated had O-H groups, which indicated the

presence of acid and alcohol structures.

6. The adsorption studies showed that the highest amount of adsorption occurred in biochar with the highest surface area, which was produced with a pyrolysis temperature of 700 °C and a holding time of 3 h. The biochar adsorbed 44.5% of the Pb^{2+} and 38.3% of the Cd^{2+} in solution, which signified its ability to be a potential choice for the sorption of these heavy metals from the environment.

ACKNOWLEDGEMENTS

The funding for this study was provided by the Central Financial Forestry Science and Technology Promotion Demonstration Project (Min[2018]TG15), and the Fujian Science and Technology Major Project (2017NZ0001).

REFERENCES CITED

Ahmad, M., Lee, S. S., Lee, S. E., Al-Wabel, M. I., Tsang, D. C. W., and Ok, Y. S. (2017). "Biochar-induced changes in soil properties affected immobilization/ mobilization of metals/metalloids in contaminated soils," *Journal of Soils and Sediments* 17(3), 717-730. DOI: 10.1007/s11368-015-1339-4

Ahmad, Z., Gao, B., Mosa, A., Yu, H., Yin, X., Bashir, A., Ghoveisi, H., and Wang, S. (2018). "Removal of Cu(II), Cd(II) and Pb(II) ions from aqueous solutions by biochars derived from potassium-rich biomass," *Journal of Cleaner Production* 180, 437-449. DOI: 10.1016/j.jclepro.2018.01.133

Angin, D. (2013). "Effect of pyrolysis temperature and heating rate on biochar obtained from pyrolysis of safflower seed press cake," *Bioresource Technology* 128, 593-597. DOI: 10.1016/j.biortech.2012.10.150

APHA 4500-P (1998). "Standard methods for the examination of water and wastewater," American Public Health Assossication, Washington, D.C.

ASTM E1755-01 (2015). "Standard test method for ash in biomass," ASTM International, West Conshohocken, PA.

Beiyuan, J., Awad, Y. M., Beckers, F., Tsang, D. C. W., Ok, Y. S., and Rinklebe, J. (2017). "Mobility and phytoavailability of As and Pb in a contaminated soil using pine sawdust biochar under systematic change of redox conditions," *Chemosphere* 178, 110-118. DOI: 10.1016/j.chemosphere.2017.03.022

Bergeron, S. P., Bradley, R. L., Munson, A., and Parsons, W. (2013). "Physico-chemical and functional characteristics of soil charcoal produced at five different temperatures," *Soil Biology and Biochemistry* 58, 140-146. DOI: 10.1016/j.soilbio.2012.11.017

Bian, R., Ma, B., Zhu, X., Wang, W., Li, L., Joseph, S., Liu, X., and Pan, G. (2016). "Pyrolysis of crop residues in a mobile bench-scale pyrolyser: Product characterization and environmental performance," *Journal of Analytical and Applied Pyrolysis* 119, 52-59. DOI: 10.1016/j.jaap.2016.03.018

Brodowski, S., Amelung, W., Haumaier, L., Abetz, C., and Zech, W. (2005). "Morphological and chemical properties of black carbon in physical soil fractions as revealed by scanning electron microscopy and energy-dispersive X-ray

spectroscopy," *Geoderma* 128(1-2), 116-129. DOI: 10.1016/j.geoderma.2004.12.019

Cantrell, K. B., Hunt, P. G., Uchimiya, M., Novak, J. M., and Ro, K. S. (2012). "Impact of pyrolysis temperature and manure source on physicochemical characteristics of biochar," *Bioresource Technology* 107, 419-428. DOI: 10.1016/j.biortech.2011.11.084

Cao, X., Ma, L., Gao, B., and Harris, W. (2009). "Dairy-manure derived biochar effectively sorbs lead and atrazine," *Environmental Science & Technology* 43(9), 3285-3291. DOI: 10.1021/es803092k

Chan, K. Y., and Xu, Z. H. (2009). "Biochar: Nutrient properties and their enhancement," in: *Biochar for Environmental Management: Science and Technology*, J. Lehmann, and S. Joseph (eds.), Earthscan, London, United Kingdom, pp. 67-84.

Chen, D., Yu, X., Song, C., Pang, X., Huang, J., and Li, Y. (2016). "Effect of pyrolysis temperature on the chemical oxidation stability of bamboo biochar," *Bioresource Technology* 218, 1303-1306. DOI: 10.1016/j.biortech.2016.07.112

Chia, C. H., Downie, A., and Munroe, P. (2015). "Characteristics of biochar: physical and structural properties," in: *Biochar for Environmental Management: Science, Technology and Implementation*, J. Lehmann, and S. Joseph (ed.),Taylor & Francis, Oxfordshire, United Kingdom, pp. 121-142

Colantoni, A., Evic, N., Lord, R., Retschitzegger, S., Proto, A. R., Gallucci, F., and Monarca, D. (2016). "Characterization of biochars produced from pyrolysis of pelletized agricultural residues," *Renewable and Sustainable Energy Reviews* 64, 187-194. DOI: 10.1016/j.rser.2016.06.003

Domingues, R. R., Trugilho, P. F., Silva, C. A., de Melo, I. C. N. A., Melo, L. C. A., Magriotis, Z. M., and Sánchez-Monedero, M. A. (2017). "Properties of biochar derived from wood and high-nutrient biomasses with the aim of agronomic and environmental benefits," *PLOS One* 12(5), 1-19. DOI: 10.1371/journal.pone.0176884

Egamberdieva, D., Hua, M., Reckling, M., Wirth, S., and Bellingrath-Kimura, S. D. (2018). "Potential effects of biochar-based microbial inoculants in agriculture," *Environmental Sustainability* 1(1), 19-24. DOI: 10.1007/s42398-018-0010-6

European Biochar Foundation (2017). *European Biochar Certificate* (Version 6.3E), European Biochar Foundation, Groningen, Holland. DOI: 10.13140/RG.2.1.4658.7043

Gascó, G., Paz-Ferreiro, J., Álvarez, M. L., Saa, A., and Méndez, A. (2018). "Biochars and hydrochars prepared by pyrolysis and hydrothermal carbonisation of pig manure," *Waste Management* 79, 395-403. DOI: 10.1016/j.wasman.2018.08.015

Ghanim, B. M., Pandey, D. S., Kwapinski, W., and Leahy, J. J. (2016). "Hydrothermal carbonisation of poultry litter: Effects of treatment temperature and residence time on yields and chemical properties of hydrochars," *Bioresource Technology* 216, 373-380. DOI: 10.1016/j.biortech.2016.05.087

Hajamini, Z., Sobati, M. A., Shahhosseini, S., and Ghobadian, B. (2016). "Waste fish oil (WFO) esterification catalyzed by sufonate activated carbon under ultrasound irradiation," *Applied Thermal Engineering* 94, 141-150. DOI: 10.1016/j.applthermaleng.2015.10.101

Han, L., Ro, K. S., Sun, K., Sun, H., Wang, Z., Libra, J. A., and Xing, B. (2016). "New evidence for high sorption capacity of hydrochar for hydrophobic organic pollutants," *Environmental Science & Technology* 50(24), 13274-13282. DOI: 10.1021/acs.est.6b02401

Inyang, M., Gao, B., Pullammanappallil, P., Ding, W., and Zimmerman, A. R.

(2010). "Biochar from anaerobically digested sugarcane bagasse," *Bioresource Technology* 101(22), 8868-8872. DOI: 10.1016/j.biortech.2010.06.088

Ippolito, J. A., Spokas, K. A., Novak, J. M., Lentz, R. D., and Cantrell, K. B. (2015). "Biochar elemental composition and factors influencing nutrient retention," in: *Biochar for Environmental Management: Science, Technology and Implementation*, J. Lehmann, and S. Joseph (ed.),Taylor & Francis, Oxfordshire, United Kingdom, pp. 139-163

Jia, Y., Shi, S., Liu, J., Su, S., Liang, Q., Zeng, X., and Li, T. (2018). "Study of the effect of pyrolysis temperature on the Cd^{2+} adsorption characteristics of biochar," *Applied Sciences* 8(7), 1-14. DOI: 10.3390/app8071019

Jin, J., Li, Y., Zhang, J., Wu, S., Cao, Y., Liang, P., Zhang, J., Wong, M. H., Wang, M., Shan, S., *et al.* (2016). "Influence of pyrolysis temperature on properties and environmental safety of heavy metals in biochars derived from municipal sewage sludge," *Journal of Hazardous Materials* 320, 417-426. DOI: 10.1016/j.jhazmat.2016.08.050

Jindo, K., Mizumoto, H., Sawada, Y., Sanchez-Monedero, M. A., and Sonoki, T. (2014). "Physical and chemical characterization of biochars derived from different agricultural residues," *Biogeosciences* 11(23), 6613-6621. DOI: 10.5194/bg-11-6613-2014

Joseph, S. D., Camps-Arbestain, M., Lin, Y., Munroe, P., Chia, C. H., Hook, J., van Zwieten, L., Kimber, S., Cowie, A., Singh, B. P., *et al.* (2010). "An investigation into the reactions of biochar in soil," *Australian Journal of Soil Research* 48(7), 501-515. DOI: 10.1071/sr10009

Kang, S.-W., Kim, S.-H., Park, J.-H., Seo, D.-C., Ok, Y. S., and Cho, J.-S. (2018). "Effect of biochar derived from barley straw on soil physicochemical properties, crop growth, and nitrous oxide emission in an upland field in South Korea," *Environmental Science and Pollution Research* 25(26), 25813-25821. DOI: 10.1007/s11356-018-1888-3

Keiluweit, M., Nico, P. S., Johnson, M. G., and Kleber, M. (2010). "Dynamic molecular structure of plant biomass-derived black carbon (Biochar)," *Environmental Science & Technology* 44(4), 1247-1253. DOI: 10.1021/es9031419

Kloss, S., Zehetner, F., Dellantonio, A., Hamid, R., Ottner, F., Liedtke, V., Schwanninger, M., Gerzabek, M. H., and Soja, G. (2012). "Characterization of slow pyrolysis biochars: effects of feedstocks and pyrolysis temperature on biochar properties," *Journal of Environment Quality* 41(4), 990-1000. DOI: 10.2134/jeq2011.0070

Kuzyakov, Y., Bogomolova, I., and Glaser, B. (2014). "Biochar stability in soil: Decomposition during eight years and transformation as assessed by compound-specific 14C analysis," *Soil Biology and Biochemistry* 70, 229-236. DOI: 10.1016/j.soilbio.2013.12.021

Lehmann, J., and Joseph, S. (2015). *Biochar for Environmental Management: Science, Technology and Implementation* (2nd Ed.), Earthscan, London, UK.

Li, K.-Q., Wang, Y.-J., Yang, M.-R, Zhu, Z.-Q., and Zheng, Z. (2014). "Adsorption kinetics and mechanism of lead(II) on polyamine-functionalized mesoporous activated carbon," *Environmental Science* 35(8), 3198-3205. DOI: 10.13227/j.hjkx.2014.08.051

Li, R., Chen, D., Liu, L., Pan, G., Chen, J., and Guo, H. (2015). "Adsorption of Pb^{2+} and Cd^{2+} in aqueous solution by biochars derived from different crop residues," *Journal of Agro-Environment Science* 34(5), 1001-1008. DOI: 10.11654/jaes.2015.05.025

Li, S., and Chen, G. (2018). "Thermogravimetric, thermochemical, and infrared spectral characterization of feedstocks and biochar derived at different pyrolysis temperatures," *Waste Management* 78, 198-207. DOI: 10.1016/j.wasman.2018.05.048

Li, S., Barreto, V., Li, R., Chen, G., and Hsieh, Y. P. (2018). "Nitrogen retention of biochar derived from different feedstocks at variable pyrolysis temperatures," *Journal of Analytical and Applied Pyrolysis* 133, 136-146. DOI: 10.1016/j.jaap.2018.04.010

Li, L., Zou, D., Xiao, Z., Zeng, X., Zhang, L., Jiang, L., Wang, A., Ge, D., and Liu, F. (2019). "Biochar as a sorbent for emerging contaminants enables improvements in waste management and sustainable resource use," *Journal of Cleaner Production* 210, 1324 -1342. DOI: 10.1016/j.jclepro.2018.11.087

Liang, B., Lehmann, J., Solomon, D., Kinyangi, J., Grossman, J., O'Neill, B., Skjemstad, J. O., Thies, J., Luizão, F. J., Petersen, J., *et al.* (2006). "Black carbon increase cation exchange capacity in soils," *Soil Science Society of America Journal* 70(5), 1719-1730. DOI: 10.2136/sssaj2005.0383

Liu, X. Y., Zhang, A., Ji, C., Joseph, S., Bian, R., Li, L., Pan, G., and Paz-Ferreiro, J. (2013). "Biochar's effect on crop productivity and the dependence on experimental conditions-a meta-analysis of literature data," *Plant and Soil* 373(1-2), 583-594. DOI: 10.1007/s11104-013-1806-x

Liu, X., Zhang, Y., Li, Z., Feng, R., and Zhang, Y. (2014). "Characterization of corncob-derived biochar and pyrolysis kinetics in comparison with corn stalk and sawdust," *Bioresource Technology* 170, 76-82. DOI: 10.1016/j.biortech.2014.07.077

Mašek, O., Brownsort, P., Cross, A., and Sohi, S. (2013). "Influence of production conditions on the yield and environmental stability of biochar," *Fuel* 103, 151-155. DOI: 10.1016/j.fuel.2011.08.044

Mechler, M. A. A., Jiang, R. W., Silverthorn, T. K., and Oelbermann, M. (2018). "Impact of biochar on soil characteristics and temporal greenhouse gas emissions: A field study from southern Canada," *Biomass and Bioenergy* 118, 154-162. DOI: 10.1016/j.biombioe.2018.08.019

Melo, L. C. A, Coscione, A. R., Abreu, C. A., Puga, A. P., and Camargo, O. A. (2013). "Influence of pyrolysis temperature on cadmium and zinc sorption capacity of sugar cane straw-derived biochar," *BioResources* 8(4), 4992-5004. DOI: 10.15376/biores.8.4.4992-5004

Mukherjee, A., Zimmerman, A. R., and Harris, W. (2011). "Surface chemistry variations among a series of laboratory-produced biochars," *Geoderma* 163(3-4), 247-255. DOI: 10.1016/j.geoderma.2011.04.021

Novak, J. M., Busscher, W. J., Laird, D. L., Ahmedna, M., Watts, D. W., and Niandou, M. A. S. (2009). "Impact of biochar amendment on fertility of a southeastern coastal plain soil," *Soil Science* 174(2), 105-112. DOI: 10.1097/SS.0b013e3181981d9a

O'Laughlin, J., and Mcelligott, K. (2009). "Biochar for environmental management: Science and technology, Johannes Lehmann Stephen M. Joseph (Eds.), Earthscan, London, UK (2009), 448 p," *Forest Policy and Economics* 11(7), 535-536. DOI: 10.1016/j.forpol.2009.07.001

Pignatello, J. J., Mitch, W. A., and Xu, W. (2017). "Activity and Reactivity of Pyrogenic Carbonaceous Matter toward Organic Compounds", *Environmental Science Technology* 51(16), 8893-8908. DOI: 10.1021/acs.est.7b01088

Sardella, F., Gimenez, M., Navas, C., Morandi, C., Deiana, C., and Sapag, K. (2015). "Conversion of viticultural industry wastes into activated carbons for removal of lead and cadmium," *Journal of Environmental Chemical Engineering* 3(1), 253-260. DOI:

10.1016/j.jece.2014.06.026

Sarfraz, R., Li, S., Yang, W., Zhou, B., and Xing, S. (2019). "Assessment of physicochemical and nutritional characteristics of waste mushroom substrate biochar under various pyrolysis temperatures and times," *Sustainability* 11(1), 277-289. DOI: 10.3390/su11010277

Song, W., and Guo, M. (2012). "Quality variations of poultry litter biochar generated at different pyrolysis temperatures," *Journal of Analytical and Applied Pyrolysis* 94, 138-145. DOI: 10.1016/j.jaap.2011.11.018

Subedi, R., Taupe, N., Ikoyi, I., Bertora, C., Zavattaro, L., Schmalenberger, A., Leahy, J. J., and Grignani, C. (2016). "Chemically and biologically-mediated fertilizing value of manure-derived biochar," *Science of The Total Environment* 550, 924-933. DOI: 10.1016/j.scitotenv.2016.01.160

Sun, J.-P., Wu, Z., Li, X., Sun, H., Ding, Y., Ping, W., and Li, Y. (2016). "Analysis of China's flue-cured tobacco planting areas and main varieties in the 21st century," *Chinese Tobacco Science* 37(3), 86-92. DOI: 10.13496/j.issn.1007-5119.2016.03.015

Sun, Y., Gao, B., Yao, Y., Fang, J., Zhang, M., Zhou, Y., Chen, H., and Yang, L. (2014). "Effects of feedstock type, production method, and pyrolysis temperature on biochar and hydrochar properties," *Chemical Engineering Journal* 240, 574-578. DOI: 10.1016/j.cej.2013.10.081

Tekin, K., Akalin, M. K., Uzun, L., Karagöz, S., Bektaş, S., and Denizli, A. (2016). "Adsorption of Pb(II) and Cd(II) ions onto dye attached sawdust," *CLEAN - Soil, Air, Water* 44(4), 339-344. DOI: 10.1002/clen.201500222

Uzun, B. B., Apaydin-Varol, E., Ateş, F., Özbay, N., and Pütün, A. E. (2010). "Synthetic fuel production from tea waste: Characterisation of bio-oil and bio-char," *Fuel* 89(1), 176-184. DOI:10.1016/j.fuel.2009.08.040

Wang, H., Xia, W., and Lu, P. (2017). "Study on adsorption characteristics of biochar on heavy metals in soil," *Korean Journal of Chemical Engineering* 34(6), 1867-1873. DOI: 10.1007/s11814-017-0048-7

Wang, Y., Yin, R., and Liu, R. (2014a). "Characterization of biochar from fast pyrolysis and its effect on chemical properties of the tea garden soil," *Journal of Analytical and Applied Pyrolysis* 110, 375-381. DOI: 10.1016/j.jaap.2014.10.006

Wang, Y-J., Bi, Y-Y., and Gao, C-Y. (2010). "Collectable amounts and suitability evaluation of straw resource in China," *Scientia Agricultura Sinica* 43(9), 1852-1859. DOI: 10.3864/j.issn.0578-1752.2010.09.011

Wang, Z., Han, L., Sun, K., Jin, J., Ro, K. S., Libra, J. A., Liu, X., and Xing, B. (2016). "Sorption of four hydrophobic organic contaminants by biochars derived from maize straw, wood dust and swine manure at different pyrolytic temperatures," *Chemosphere* 144, 285-291. DOI: 10.1016/j.chemosphere.2015.08.042

Wang, Z., Liu, G., Xing, M., Li, F., and Zheng, H. (2014b). "Cd (II) adsorption characteristics of biochar at different pyrolysis temperatures," *Environmental Science* 35(12), 4735-4744. DOI: 10.13227/j.hjkx.2014.12.042

Windeatt, J. H., Ross, A. B., Williams, P. T., Forster, P. M., Nahil, M. A., and Singh, S. (2014). "Characteristics of biochars from crop residues: Potential for carbon sequestration and soil amendment," *Journal of Environmental Management* 146, 189-197. DOI: 10.1016/j.jenvman.2014.08.003

Wu, W., Yang, M., Feng, Q., McGrouther, K., Wang, H., Lu, H., and Chen, Y. (2012). "Chemical characterization of rice straw-derived biochar for soil amendment," *Biomass and Bioenergy* 47, 268-276. DOI:

10.1016/j.biombioe.2012.09.034

Xiao, R., Wang, J. J., Gaston, L. A., Zhou, B., Park, J.-H., Li, R., Dodla, S. K., and Zhang, Z. (2018). "Biochar produced from mineral salt-impregnated chicken manure: Fertility properties and potential for carbon sequestration," *Waste Management* 78, 802-810. DOI: 10.1016/j.wasman.2018.06.047

Yan, X., Liu, X., Qiao, K., Wang, Y., and Zhai, Z. (2008). "Research progress of technology for forming activated carbon," *Progress in Chemical Engineering* 27(12), 1868-1872. DOI: 10.3321/j.issn:1000-6613.2008.12.002

Yin, Y., Zhang, P., Lei, H., Ma, H., and Gao, Ren (2014). "Effects of different pyrolysis temperatures on the chemical properties of biomass carbon," *Journal of Tropical Crops* 35(8), 1496-1500. DOI: 10.3969/j.issn.1000-2561.2014.08.008

Yoo, J.-C., Beiyuan, J., Wang, L., Tsang, D. C. W., Baek, K., Bolan, N. S., Ok, Y. S., and Li, X.-D. (2018). "A combination of ferric nitrate/EDDS-enhanced washing and sludge-derived biochar stabilization of metal-contaminated soils," *Science of the Total Environment* 616-617, 572-582. DOI: 10.1016/j.scitotenv.2017.10.310

Yuan, J.-H., Xu, R.-K., and Zhang, H. (2011). "The forms of alkalis in the biochar produced from crop residues at different temperatures," *Bioresource Technology* 102(3), 3488-3497. DOI: 10.1016/j.biortech.2010.11.018

Zhang, C. (2002). "Current status and prospects of tobacco rod resource utilization technology," *Research on Renewable Resources* 1, 38-39. DOI: 10.3969/j.issn.1674-0912.2002.01.013

Zhang, C., He, C, and Qiao, Y. (2018). "Lower-temperature pyrolysis to prepare biochar from agricultural wastes and Adsorption for Pb^{2+}," *BioResources* 13(3), 5543-5553. DOI: 10.15376/biores.13.3.5543-5553

Zhang, J., Liu, J., and Liu, R. (2015). "Effects of pyrolysis temperature and heating time on biochar obtained from the pyrolysis of straw and lignosulfonate," *Bioresource Technology* 176, 288-291. DOI: 10.1016/j.biortech.2014.11.011

Zhang, Y., Shao, M., Lin, Y., Luan, S., Mao, N., Chen, W., and Wang, M. (2013). "Emission inventory of carbonaceous pollutants from biomass burning in the Pearl River Delta Region, China," *Atmospheric Environment* 76, 189-199. DOI: 10.1016/j.atmosenv.2012.05.055

Zhao Z., Ibrahim, M. M., Wang, X., Xing, S., Heiling, M., Hood-Nowotny, R., Tong, C., and Mao, Y. (2019). "Properties of biochar derived from spent mushroom substrates," *BioResources* 14(3), 5254-5277. DOI: 10.15376/biores.14.3.5254-5277

Zhao, S., Ji, Q., Li, Z., and Wang, X. (2015). "Characteristics and mineralization in soil of apple-derived biochar produced at different temperatures," *Transactions of the Chinese Society for Agricultural Machinery* 46(6), 183-192. DOI: 10.6041/j.issn.1000-1298.2015.06.026

Zhu, B., Zhou, Y., and Wang, W. (2016). "Kinetic and isotherm of lead adsorption by reed straw biochar," *Hydrometallurgy of China* 35(4), 297-303. DOI: 10.13355/j.cnki.sfyj.2016.04.006

Zhu, J.-M., Wang, Z.-W., Gao, J.-H., Xie, C.-R., Zhang, H.-Y., Xie, X.-Y., and Jin, C. (2017). "Adsorption characteristics of vegetable waste-based biochar for lead," *Journal of Safety and Environment* 17(1), 232-239. DOI: 10.13637/j.issn.1009-6094.2017.01.045

Zienlińska, A., and Oleszczuk, P. (2015). "Evaluation of sewage sludge and slow pyrolyzed sewage sludge-derived biochar for adsorption of phenanthrene and pyrene," *Bioresource Technology* 192, 618-626. DOI:

10.1016/j.biortech.2015.06.032
Zou, F., He, C., Zhang, Y., Shi, H., and Kai, Z. (2018). "Comparison of the adsorption of Pb^{2+} by biochar of five crop straw," *Journal of Materials Science and Engineering* 36(6), 137-141. DOI: 10.14136/j.cnki.issn1673-2812.2018.06.025

Article submitted: Jan. 3, 2020; Peer review completed: April 3, 2020; Revised version received and accepted: April 7, 2020; Published: April 10, 2020.
DOI: 10.15376/biores.15.2.4026-4051